



Performance evaluation and thermal analysis of pottery furnace in Thimi, Bhaktapur

Ushan Adhikari^a, Bijendra Prajapati^b and Anil Mani Bhandari^{a,*}

^aDepartment of Automobile and Mechanical Engineering, Thapathali Campus, Institute of Engineering, Tribhuvan University, Kathmandu, Nepal

^bDepartment of Mechanical and Aerospace Engineering, Pulchowk Campus, Institute of Engineering, Tribhuvan University, Lalitpur, Nepal

ARTICLE INFO

Article history:

Received 11 Sep 2021
Received in revised form
07 Dec 2021
Accepted 09 Dec 2021

Keywords:

Furnace design
CFD simulation
Furnace modeling
Pottery production
Performance analysis

Abstract

Pottery is a unique art that involves creating items out of clay. It creates a variety of clay and ceramic products, including as flowerpots, water and grain storage jars, by distilling rice spirits. Almost all pottery manufacture is done in the conventional manner, which uses more energy and emits hazardous emissions. This project primarily focuses on experimental performance analysis, calculating temperature distribution, fuel required per batch, pottery production per batch, maximum temperature reading, flame temperature, and energy audit for an existing furnace and thermal analysis of pottery furnace giving optimum design for future construction and modification of existing furnace. Energy calculation shows that specific fuel consumption of different furnaces in Thimi varies from 0.98MJ/kg to 2.4MJ/kg. Experimental data are collected and validated by transient thermal analysis using ANSYS.

©JIEE Thapathali Campus, IOE, TU. All rights reserved

1. Introduction

Thimi is known for traditional handicrafts and pottery products. This boasts one of the oldest and longest-running handcraft pottery businesses. This article mainly focuses on the performance evaluation of the existing pottery furnaces based on Temperature distribution, fuel consumption, and time-temperature relationship in Thimi, Bhaktapur, Nepal.


Earthenware, stoneware, and porcelain are some of the most common varieties of pottery wares. An item must be fired ceramic ware that contains clay when produced to be considered pottery [1]. The amount of energy required for chemical changes was minimal, but the amount of energy consumed in heating the pottery and the furnace structure was substantial, and this energy was lost when the furnace and products were allowed to cool before being retrieved for use [2]. The flue gases are extracted via a porous floor with flues underneath

(downdraft) [2]. Since the traditional pottery-making process is energy, labor-intensive, and emits harmful emissions to the environment, therefore, research is now focusing on minimizing emission and increasing production efficiencies.

Cultural determinism is a fundamental assumption in traditional archaeological pottery analysis: that the nature of a pottery vessel is dictated by cultural pressures, that forms, decorations, and functions reflect cultural learning, and that classification of these characteristics of pottery corresponds to a cultural classification [3].

Pottery has always been seen as a utilitarian or symbolic-votive item throughout history. Its importance in the formation and replication of social connections and cultural values is generally acknowledged in social sciences as well. Several writers argue that, when all other variables are taken into account, technology can be influenced by behavioral or socio-cultural elements such as ideology, religion, or ethnicity [4].

*Corresponding author:

 bhandari.amb@gmail.com (A.M. Bhandari)

As shown in Figure 1, in open type furnace, pots are stacked up, covered with straw and ash, and then burned in a smoky firing. Smoke and ash billow through the town's streets. When the fire subsides and the ash is swept away, the pots are left to cool. After the firing process, those pots used to be carried around to different villages in yokes and were sold door-to-door. Today most potters transport by vehicles. The proximity of the potters' workshops to one another has created a working environment of cooperation that has existed for hundreds of years in the village.



Figure 1: Traditional open firing process

Pottery is unique in that it provides a wealth of information on the extraction, processing, adjustments, and firing of raw materials during the manufacturing process. Ceramics are the most essential items for learning international style and connections because they combine tradition with style and technology to reflect many elements of life in this culture. The transfer of techniques was influenced by technological know-how [5].

To get the required color, potters burned creamware pottery, which was made with glauconite-bearing fossiliferous carbonate clay, at 800–850 °C in an updraft kiln in an oxidizing environment [6].

The design parameters are (a) geometric aspect ratio (D/H) and (b) refractory thickness (L). Based on the model's findings, it was discovered that: (a) furnaces with higher aspect ratios (D/H) are superior to furnaces with lower aspect ratios [7].

A temperature of 900°C is required for the decomposition of clay to amorphous silica and alumina, which is the optimum temperature in the traditional pottery business. The highest temperature attained is sufficient to remove both free and chemically bound water and the results of the water evaporation model in CFD support this [8].

The temperature in the furnace fluctuates substantially, which influences the quality of the clay bodies owing

to the possibility of cracking. Because the influence of radiation in heat transmission is minimized when clay bodies are packed compactly in the furnace, the danger of cracks is also affected [8]. The evaporation model can also be simulated, although some issues are owing to the quick pace of reactions; nevertheless, with stronger assumptions and more precise calculations, the conclusion would be even more reliable [8].

Compression testing of ceramics is terrifying: specimens crack with terrifying noises and fly apart into little shards; certain materials even generate lightning flashes. The pieces leave a significant imprint on the anvil's surfaces [9].

There are numerous steps to clay processing in the traditional pottery industry. To minimize pollution and manufacturing round time, the method and quality of the pottery must be improved, which may be accomplished by enhancing the heating process. Turbulent three-dimensional numerical simulations of the in-use air intake and a redesigned design are used to achieve this aim [10].

The downdraft kiln was created to replace the European bottle updraft kiln. Its design provided inherently even temperature, the ability to control temperature distribution and atmosphere, low fuel consumption, and the ability to expand the kiln to an extremely large size while maintaining the firing characteristics of a smaller kiln [11].

2. Methods and methodology

2.1. Data collection

At first, the site for the study is selected, detailed data from the five selected sites are taken.



Figure 2: Temperature measurement

Figure 2 indicates the picture of temperature measurement at Bahakha and Digu Tole. Data collected are temperature distribution concerning height and side.

The maximum and minimum temperature recorded inside the furnace, outside furnace, flame temperature. Besides temperature, the weight of pottery product before and after firing, the weight of fuel (wood) used are measured. These data and calorific values measured in the lab are used to evaluate the performance of the furnace.

The infrared thermometer gun was used for collecting the temperature data required for performance analysis. To study the temperature distribution in the furnaces i.e., both open type and close type furnaces, attempts have been made to read the temperature distribution using Amprobe IR-730 Thermal gun. It can measure temperature in between -32°C to 1050°C . The readings have been carried out separately for open-type and closed-type furnaces. For the temperature distribution profile study, all four sides (where possible) have been selected with 6 to 9 points on each side as shown in the figure that is equally spaced.

A combustion analyzer also called a flue gas analyzer is an essential tool for detailed analysis of combustion processes in boilers, furnaces, heaters, and any application using a combustion process, including gas, petrol, and diesel engines. We can supply a wide range of flue gas and combustion analyzers for the detection of various gases, which indicate problems in the combustion process, and can verify that the process is both complete and efficient. The combustion gas analyzer used for the measurement of flue gas characteristics, and picture taken while data being collected is shown in Figure 3.



Figure 3: Reading taking from flue gas meter

In the closed type furnace, the gas analyzer had shown the readings as in Table 1.

Whereas, an open-type furnace gas analyzer shows the readings as in Table 2.

Table 1: Chemical Composition (%) of cement and waste marble dust

SN	Particulars	Closed Type Furnace		
		Site A Bahakha Bazaar	Site B Nasnani	Site C Diguli Lower
1	O ₂	10.30%	9.20%	15.80%
2	CO (ppm)	1238	14060	3660
3	CO ₂	9.60%	10.60%	4.60%
4	T Flue	290.70C	920C	54.500C
5	T air	15.80C	21.20C	18.10C
6	dT	274.90C	70.80C	36.40C
7	Excess air	97%	79%	310%
8	NO	78ppm	63ppm	25ppm
9	NO ₂	0ppm	1ppm	0ppm
10	NO _x	78ppm	64ppm	25ppm
11	Draft	0.2mm	2mm	0.5mm
		H ₂ O	H ₂ O	H ₂ O

Table 2: Details of mixing criteria

SN	Particulars	Open Type Furnace		
		2 nd Day	3 rd Day	4 th Day
1	O ₂	14.60%	10.40%	20.90%
2	CO (ppm)	16659	15310	12
3	CO ₂	6.20%	10.30%	0%
4	T Flue	63.70C	69.30C	62.50C
5	T air	20.20C	15.3 0C	15.40C
6	dT	43.50C	540C	47.10C
7	Excess air	232%	99%	-
8	NO	70ppm	28 ppm	1ppm
9	NO ₂	0ppm	0 ppm	0 ppm
10	NO _x	70ppm	28 ppm	1 ppm
11	Draft	0.2mm	0.3mm	0.6mm
		H ₂ O	H ₂ O	H ₂ O

2.2. Case study 1: Bahakha

In Bahakha site, 744.32 kg of raw pottery product is fired to its final product with 336kg of wood. And temperature distribution outside the wall is recorded in two terms one is according to height and another is according to side of the furnace wall.

The Figure 4 shows the rate of temperature increment of the outside wall over the firing period. During the period temperature drop seen is due to the burner position of the fire on the frontal area. Since fire flame comes out of burning area and increases the wall temperature.

In Figure 5 sidewise temperature distribution shows the increment rate is smooth, however, at some points temperature seems to fluctuate instead of constant increment rate. This is because the flame was coming out of the burning area and increasing the wall temperature steeply and cools down later and the overall temperature of the wall had been increased.

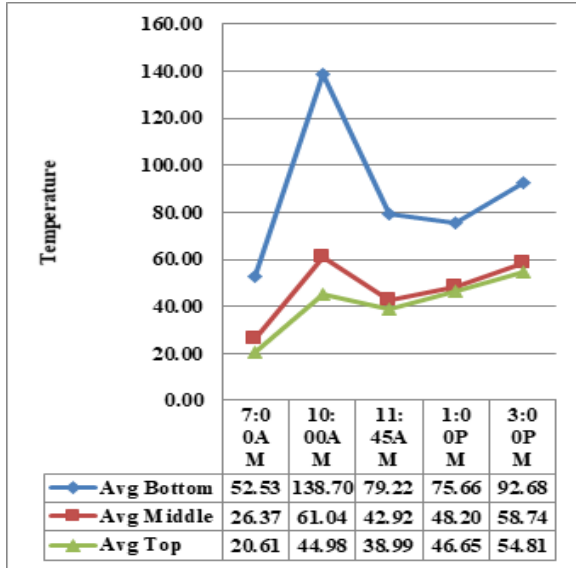


Figure 4: Temperature v/s Time (Height Variation) of Bahakha site

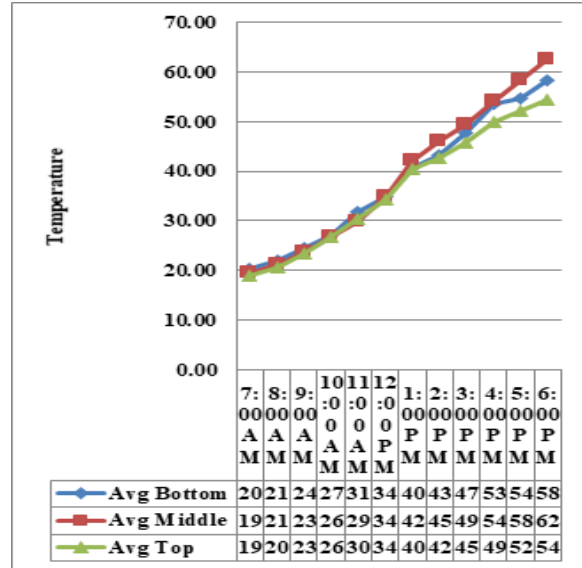


Figure 6: Temperature v/s Time (Height Variation) of Bahakha site

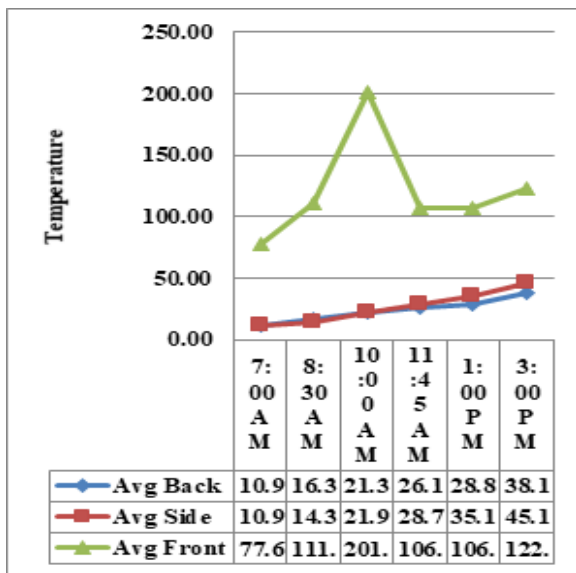


Figure 5: Temperature v/s Time (Side Variation) of Bahakha site

The average temperature of the kiln measured at a different height at a different time of day is plotted as. The result shows uniform temperature along with the height of the kiln. Temperature increases uniformly from 21°C to 58°C during the process.

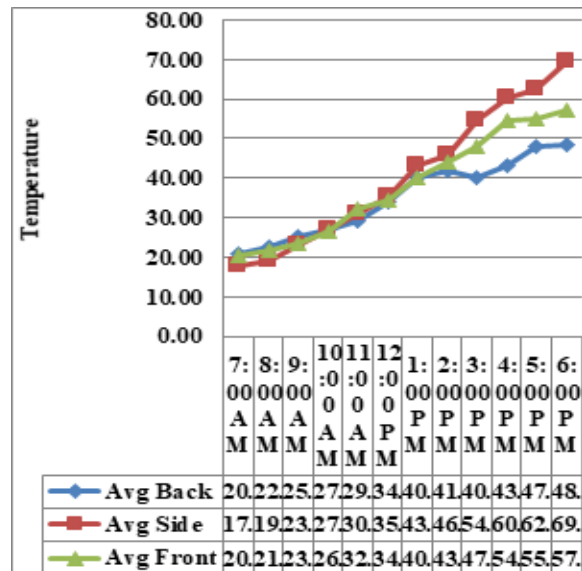


Figure 7: Temperature v/s Time (Side Variation) of Bahakha site

2.3. Case study 2: Digu Tole

In Digu Tole, 2538.81 kg of raw pottery product is fired with 464 kg of fuel (wood) to its final product. The final product weighs 2264.33 kg.

Figure 6 shows the average temperature based on the side of the furnace is found on the side of the furnace. This indicates that the flame has not come out of the burning area and insulation on the side seems quite low.

Although some variation was seen in some point of time as shown in Figure 7, the average calculation shows the increasing rate in the different side of the wall. The average temperature of the side of the wall is maximum

is because of the furnace structure (two furnace rooms in a single furnace) and wall thickness near to the burning area.

2.4. Case study 3: Nasnani

In Nasnani, 2259.735 kg of raw potter product is fired with 412.71 kg of wood in 660 min and its final product weighs 1941.355 kg. The temperature distribution of the furnace is as follows.

As shown in Figure 8 Average temperature of the existing furnace Nasnani had an almost even temperature distribution. However, each side has a different rate of increment. The Frontal part of the furnace has a higher temperature in comparison to the other side's temperature is obvious as the front part of the furnace faces direct contact with the fire flame as the firing hole is at the front and backside of the furnace.

Figure 9 indicates an increment of temperature versus height of the furnace. The average temperature of the bottom is higher which is an obvious result as the burning starts from the bottom of the furnace. Overall, the temperature is increasing and almost evenly distributed.

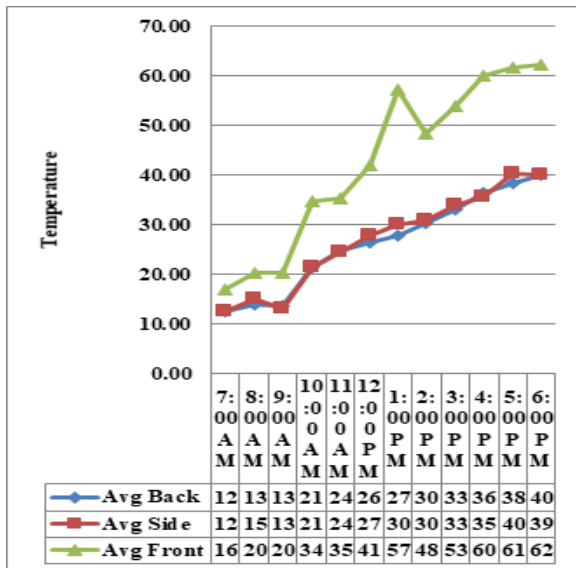


Figure 8: Temperature v/s Time (Side Variation) of Nasnani site

2.5. Specific fuel consumption

Three sites are mainly studied for final calculations of the energies and comparative performance. Following data as shown in Table 3 are calculated based on experimental data.

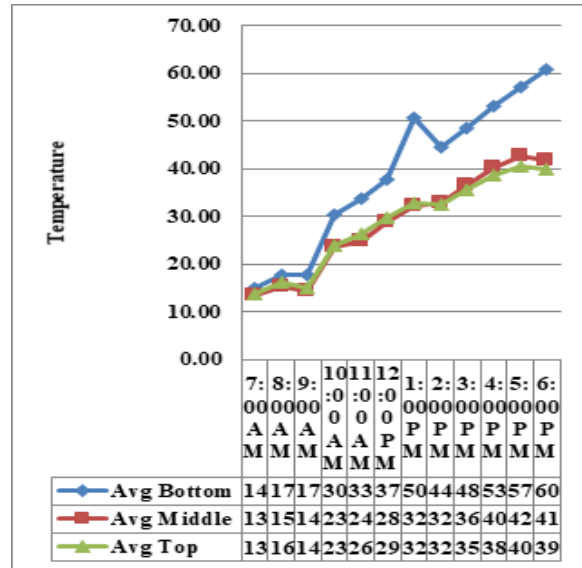


Figure 9: Temperature v/s Time (Height Variation) of Nasnani site

3. CFD theory

Computational fluid dynamics (CFD) is a software tool for numerically solving the Navier Stokes equation (N.S). Differential equations that explain the motion of a fluid are known as N.S. Equations. For solving momentum, heat, and mass transport for a given shape, CFD employs N.S. Equations. The geometry is divided into computation cells, and then N.S. Iteratively, equations are solved numerically for each cell. The quality of the geometry resolution, input data, and program knowledge all have a major impact on the outcome. Typically, computer capacity is a stumbling block. The data can provide a picture of the temperature distribution and flow field, but they must be scrutinized. CFD has the benefit of being able to quickly obtain a thorough understanding of a system. As a result, CFD is highly beneficial for both current systems and preliminary investigations of future system functionality. The performance of a new design of a downdraught kiln is practically expensive and nearly difficult to study in this project. As a result, utilizing CFD computer models to conduct a thermal study of new downdraught kilns is sometimes the most feasible method.

3.1. Governing transport equation

To solve fluid flows, several assumptions must be established. This assumption simplifies the equation by making the flow incompressible, which is defined as no fluctuation in density along the streamline of continuity to Equation 1. The flow is also assumed to be considered a Newtonian fluid. The viscous stress of a Newtonian

Table 3: Details of mixing criteria

Description	Bahakha	Digu Tole	Nasnani
No of pottery products fired in one batch	536	1054	1049
Average weight of fired pottery product (kg)	1.388	2.4	2.25
Total weight of fired batch (kg) before firing	744.32	2538.81	2259.73
Total weight of fired batch (kg) after firing	644.86	2264.31	1941.36
Type of fuel: Eucalyptus branches	Hardwood chips	Hardwood chips	Hardwood chips
Weight of fuel used in one batch	336	556.92	412.71
Moisture content in fuel at pottery furnace site (%)	9.60	9.60	9.60
Moisture content in fuel at which GCV was measure in lab	-	-	-
GCV of fuel measure in lab (MJ/Kg)	4.6135	4.6135	4.6135
GCV of fuel at the moisture level at pottery furnace site : GCV of fuel measured in lab X(MJ/Kg)	4.6135	4.6135	4.6135
Total energy input : GCV of fuel at pottery furnace site X Weight of fuel used	1550.13	2565.1	1904.04
Specific energy consumption: MJ/Kg fired pottery product	2.403	1.133	0.981

fluid is a linear function of the rate of strain, and this is true for most common fluids like gas and water, where the viscous stress may be expressed as Equation 2. The equation of motion is expressed as an equation based on these assumptions Equation 3. The three dimensions are denoted by the letters i and j . The first term in this equation represents accumulation, the second term represents convection, the third term represents the rate of change of pressure due to motion, the fourth term represents diffusion, analyst term represents the source term [12].

$$\frac{\partial U_j}{\partial x_j} = 0 \quad (1)$$

$$\tau_{ij} = \tau_{ji} = \mu \left(\frac{\partial U_j}{\partial x_j} + \frac{\partial U_j}{\partial x_j} \right) \quad (2)$$

$$\frac{\partial U_i}{\partial t} + U_j \frac{\partial U_i}{\partial x_j} = -\frac{1}{\rho} \frac{\partial P}{\partial x_i} + \mu \frac{\partial}{\partial x_j} \left(\frac{\partial U_j}{\partial x_j} + \frac{\partial U_j}{\partial x_j} \right) + G_i \quad (3)$$

CFD software solves these equations numerically by dividing the computing domain into cells, converting partial differential equations to algebraic equations. Numerical mistakes are also caused by this reformation,

and the amount of these errors is dependent on the cell size. While a smaller cell size reduces inaccuracy, it also increases computing time, which is expensive. When dealing with CFD, you must constantly strike a balance between accuracy and cost.

3.2. Turbulence modeling

Turbulence aids mass transport and chemical reactions in industrial environments. It's fascinating from an engineering viewpoint to be able to simulate turbulence. Turbulence is a turbulent state of fluid flow that is chaotic and unpredictable. Turbulence flows are distinguished by their irregularity (different shapes and sizes), diffusivity, instability, three-dimensional formations, and kinetic energy dissipation. Because of all of these characteristics, turbulent flows are very unpredictable and difficult to model [12].

There are many different models available, each of which is based on different assumptions and has different applicability and limitations. In this study, the K-epsilon model was used.

3.3. Standard K-epsilon turbulence model

The most popular model used in computational fluid dynamics (CFD) to predict mean flow characteristics for turbulent flow conditions is the K-epsilon (k-) turbulence model. It is a two-equation model that uses two transport equations and partial differential equations to

offer a broad description of turbulence (PDEs). The K-epsilon model was created to improve the mixing-length model and find an alternative to algebraically dictating turbulent length scales in moderate to high complexity flows. Many unknown and unmeasurable terms appear in the precise k-equations. The conventional k-turbulence model is utilized for a much more practical approach, since it is based on our best knowledge of the relevant processes, minimizing unknowns and offering a set of equations that can be used to a wide range of turbulent applications. k is the kinetic energy of turbulent motion [13].

$$\frac{\partial(\rho k)}{\partial t} + \frac{\partial(\rho k u_i)}{\partial x_i} = \frac{\partial}{\partial x_j} \left[\frac{\mu_t}{\rho k} \frac{\partial k}{\partial x_j} \right] - 2\mu_t E_{ij} E_{ji} - \rho \epsilon \quad (4)$$

For dissipation ϵ

$$\frac{\partial(\rho \epsilon)}{\partial t} + \frac{\partial(\rho \epsilon u_i)}{\partial x_i} = \frac{\partial}{\partial x_j} \left[\frac{\mu_t}{\rho \epsilon} \frac{\partial \epsilon}{\partial x_j} \right] - C_{1\epsilon} \frac{\epsilon}{k} 2\mu_t E_{ij} E_{ji} - 2C_{2\epsilon} \rho \frac{\epsilon^2}{k} \quad (5)$$

Rate of change of k or ϵ in time + Transport of k or ϵ by advection = Transport of k or ϵ by diffusion + Rate of production of k or ϵ - Rate of destruction of k or ϵ

Where it represents velocity component in the corresponding direction E_{ij} represents a component of the rate of deformation μ represents eddy viscosity.

$$\mu t = \rho C \mu \frac{k^2}{\epsilon} \quad (6)$$

The equations also consist of some adjustable constants σk , $\sigma \epsilon$, $C_{1\epsilon}$ and $C_{2\epsilon}$. The values of these constants have been arrived at by numerous iterations of data fitting for a wide range of turbulent flows. These are as follows $C_{\mu} = 0.09$, $\mu k = 1.00$, $\sigma \epsilon = 1.30$, $C_{1\epsilon} = 1.44$, $C_{2\epsilon} = 1.92$ [13].

3.4. CFD modeling

Modeling the real pottery kiln, which is densely packed with clay bodies, is extremely difficult. This project's simulation model includes a basic geometry and three clay bodies. Clay bodies are roughly shaped as two types of rectangular slabs with thicknesses of 2cm and 1cm. The simulation is solely for the movement of air. The general method of working while creating the model was iterative and incremental. The mesh in the model is of high quality, especially along the walls [12].

3.5. Development of geometry

The Figure 10 shows the final geometry of the existing pottery furnace.

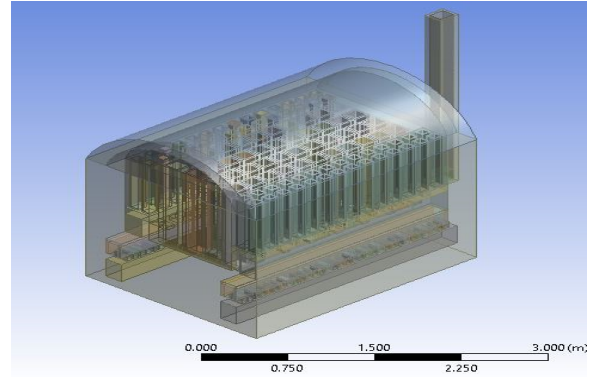


Figure 10: Temperature v/s Time (Height Variation) of Nasnani site

The geometry was created using the solid works 2020.

And imported to the ANSYS Workbench platform. To reduce the computational time, a simple model is adopted. Pottery wares are approximated as rectangular slabs of cross-section 17.5cm×17.5cm and 10cm×10cm. To reduce the computational time and increase the accuracy level, wares are simplified in geometry.

3.6. Boundary conditions

The turbulence model was used the standard k-epsilon model. Simulation is done only to see air movement. There are four inlet ports for air entrance, I assume 3m/sec inlet velocity so that the air can move from inlet port to outlet port.

3.7. Mesh

The mesh was created in the meshing tool from the ANSYS Workbench platform. The number of nodes are 44804 and the number of elements in the mesh are 148247. Figure 11 shows computer generated mesh model.

3.8. Model creation

The model creation started with the drawing of the geometry and its discretization through a meshing process. Continued with the definition of the simulation setup, and ended with the analyses of the results [14].

3.9. Making geometry

The geometry of my study is selected from one of the sites (Bahakha site). The dimension of the furnace is almost similar to the experimental furnace. Without roof dimensions, the furnace is 195 cm height × 208 cm width and 270 cm length and 3 m height of the chimney.

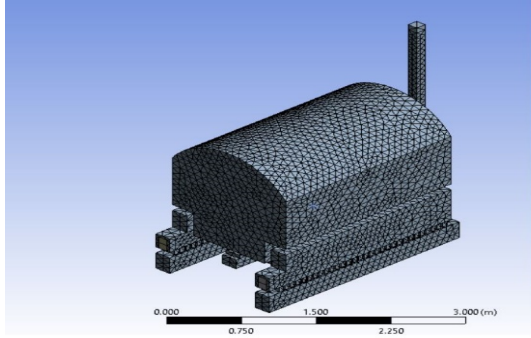


Figure 11: Meshing for the airflow simulation inside the furnace.

Dimensions represent the outer dimension; the internal dimension is about 126 cm height 162 cm width and 223cm length as shown in Table 4.

Table 4: Major dimension of model

	Height (cm)	Width (cm)	Length (cm)
Outer furnace	195	208	270
Inner furnace	126	162	223
Fire hole	24	19	270

3.10. Boundaries conditions

The boundary condition at wall boundaries was given from experimental data. The flame temperature is given as 1050-degree Celsius, thermal conductivity is assumed to be 1.44 (W/mK), and single-step time of 36000 sec. Under this condition the outer surface temperature was too large, so to compensate for the wall temperature similar to the experimental verification, ambient temperature is set to an extreme condition of -5 degrees Celsius. The obtained data is similar to the experimental data.

3.11. Dynamic mesh

The use of a dynamic mesh of size 7cm allowed us to do a transient simulation, and final meshing is as shown in the Figure 12.

4. Result and discussion

4.1. Flue gas measurement

Flue gas from open type and closed type furnaces both were measured using a flue gas analyzer. During measurement, open type furnace produced more CO ppm than closed type furnace. The maximum CO emission recorded in open type furnace is 16659 ppm whereas in closed type furnace 14060 ppm.

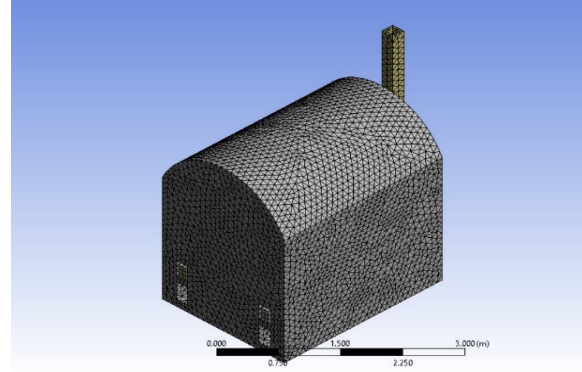


Figure 12: Final meshing for the transient thermal analysis.

4.2. Temperature measurement

Temperature measurement of the furnace is done at various predefined locations of the furnace wall. Three sites were studied in detail to find out temperature distribution outside the furnace wall. During temperature measurement the maximum temperature in average (side-wise) reached was found in the front wall this was due to flame coming out of the burning area. And maximum average temperature (height-wise) was found at the bottom. Whereas minimum temperature recorded height-wise was at the top and minimum temperature recorded side-wise was average of left and right side.

For a better pottery product, the maximum temperature inside the furnace should as much maximum as it can be reached. The maximum temperature inside a closed type furnace at the end of firing was recorded as 663.4 degrees Celsius.

4.3. Calorific values of wood

The calorific value of the fuel (wood) that was mostly used in the Thimi to burn pottery products was tested in the lab. Four different types of sample fuel such as rice husk, hardwood chips, pine chips, and straw. Among them, pine chips had a maximum calorific value of 4779.2 Kcal/kg. and minimum calorific value of fuel measured in the lab was Straw which is 3239.8 Kcal/K

4.4. Moisture content in fuel

The moisture content in the fuel also has an impact in the performance parameter of furnace efficiencies. So, the moisture content in the fuel was measured in the lab. Among rice husk, hardwood chips, pine chips, and straw, the maximum moisture content was found in the rice husk which is 12.93% and minimum moisture content was measured in hardwood chips which are 9.6%.

Besides moisture content volatile matter content, ash content, total fixed carbon content was also measured in the lab. The result is shown in the Table 5.

Table 5: Moisture content measured in the laboratory

SN	Particulars (%)	Rice Husk	Hard wood Chips	Pine Chips	Straw
1	Moisture Content	12.93	9.6	9.23	8.48
2	Volatile Matter Content	58.04	62.82	60.69	61.43
3	Ash Content	11.81	4.32	0.44	16.23
4	Total Fixed Carbon Content	17.22	23.26	29.64	13.86

4.5. Compressive strength test

The sample from the open type furnace’s product and closed type furnace’s product is taken and compressive strength was measured in the lab and the result shows that the closed type furnace’s product has more compressive strength than open type furnace. The average compressive of the closed furnace’s product is 14.10 N/mm² whereas the sample from the open type furnace’s product has an average compressive strength of 13.38 N/mm².

4.6. CFD air movement

Since the furnace is designed in such a way that the temperature distribution is uniform. The simulation result shows that the air movement is so smooth that the temperature flame can move smoothly so that the temperature will be uniform.

In the simulation, there are four inlet ports and a single outlet which is the chimney. The inlet velocity was assumed to be 3 m/sec. Besides the hurdle for air movement the room air speed is around 3m/sec in the furnace room. And inlet velocity is taken as 3m/sec and output velocity was found to be between 0-10 m/sec.

From Figure 13 and result analysis of airflow movement, almost even airflow is obtained that indicates even temperature distribution.

The period of a single step 36000 sec from the starting of the firing is applied. In particular, simulation was done in experimental boundaries condition of the furnace and validated through an experimental test done in the real furnace in Bahakha Thimi, Bhaktapur, Nepal

Figure 14 shows the final temperature recorded on the surface of the furnace in the simulation. Which is almost

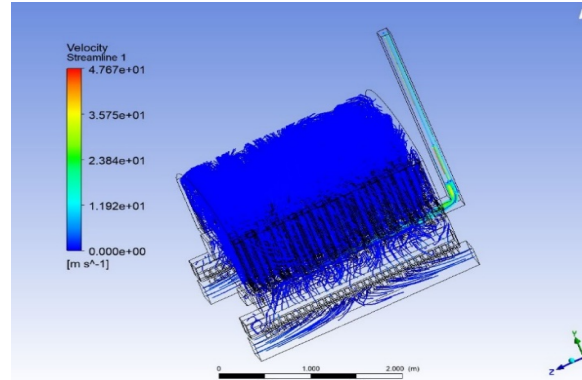


Figure 13: Airflow in CFD simulation

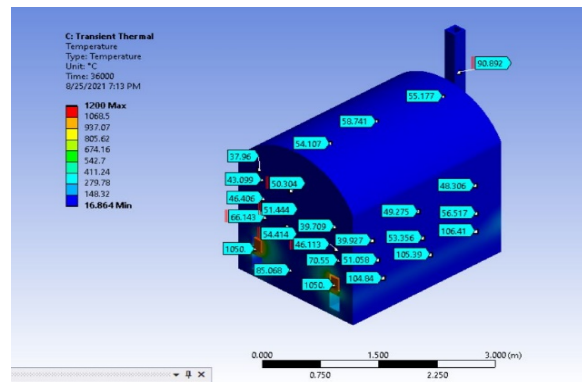


Figure 14: Final temperature distribution in transient thermal analysis

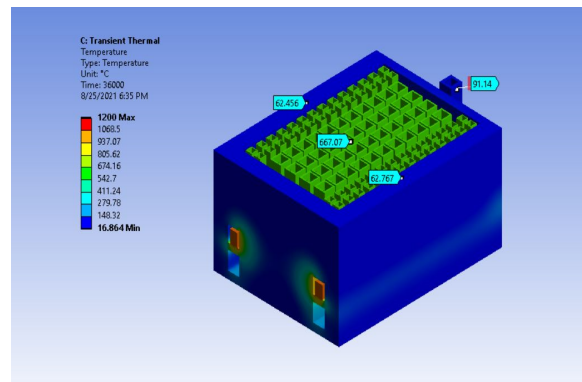


Figure 15: Cross-sectional view of the transient thermal behavior at the end of the firing

similar to the experimental temperature recorded in the Nasnani site.

Figure 15 shows the cross-sectional view of the final result of the simulated furnace and the corresponding temperature inside the furnace.

5. Conclusion

The completion of the performance analysis of the pottery furnace and thermal analysis was done by firstly collecting the temperature distribution inside and outside the furnace versus time. The experimental data are validated by transient thermal analysis. Following conclusions are drawn.

- Temperature distribution outside of the furnace wall shows that the maximum average temperature and minimum average temperature according to height were found in the bottom and top of the furnace. Whereas according to side the maximum temperature is recorded in front and backside of the wall and minimum temperature is recorded on right and left side of the wall.
- Specific fuel consumption is highest at the Bahakha site and minimum at the Nasnani site.
- Flue gas measurement shows that the emission in the open type furnace is more than that of the closed type furnace.
- Calorific value measured in the lab shows that the pine chips have maximum calorific values which are mainly used in closed type furnaces. So, closed type furnace is recommended.
- Moisture content in the different types of fuel measured in the lab shows that the risk husk possesses the highest percentage of moisture content among rice husk, hardwood chips, pine chips, and straw. Since rice husk is mostly used in the open type furnace and hence it uses low-quality fuel.
- From the lab report compressive strength of the product from the closed type furnace is more than that of the open type furnace.
- CFD flow of the air at an inlet velocity of 3m/s shows that the flame and air mixture is smoothly moving inside the furnace that indicating the uniform temperature distribution inside the furnace.
- Transient thermal analysis validates the experimental data.

6. Acknowledgement

This work has been completed under the financial assistance of the University Grant Commission (UGC), the UGC Masters Research Support Award Number is MRS-77/78-Engg-03. The authors would like to thank all supportive members of Thimi society for providing furnaces for the study.

References

- [1] Deneen Pottery. Pottery: The ultimate guide, history, getting started, inspiration[EB/OL]. 2021[2021-03-04]. <https://deneenpottery.com/pottery/>section-2.
- [2] Thimi Ceramics. Stoneware products from Thimi Nepal[EB/OL]. 2019[2021-03-08]. <https://www.thimiceramics.com/thimi-pottery/>.
- [3] Rye O S. Keeping Your Temper Under Control: Materials and the Manufacture of Papuan Pottery[J/OL]. *Archaeology and Physical Anthropology in Oceania*, 1976, 11(2): 106-137. <https://onlinelibrary.wiley.com/doi/10.1002/j.1834-4453.1976.tb00245.x>. DOI: <https://www.doi.org/10.1002/j.1834-4453.1976.tb00245.x>.
- [4] Beltrame M, Sitzia F, Liberato M, et al. Comparative pottery technology between the Middle Ages and Modern times (Santarém, Portugal)[J/OL]. *Archaeological and Anthropological Sciences*, 2020, 12(7): 130. <https://link.springer.com/10.1007/s12520-020-01053-x>. DOI: <https://www.doi.org/10.1007/s12520-020-01053-x>.
- [5] Emami M. Production of Pottery from Esfandaghe and Jiroft, Iran, late 7th - early 3rd Millennium BC[J/OL]. *Materials and Manufacturing Processes*, 2020, 35(13): 1446-1454. <https://doi.org/10.1080/10426914.2020.1752919><https://www.tandfonline.com/doi/full/10.1080/10426914.2020.1752919>. DOI: <https://www.doi.org/10.1080/10426914.2020.1752919>.
- [6] Borgers B, Ionescu C, Willems S, et al. Continuity and diversity of Roman pottery production at Famars (northern France) in the 2nd–4th centuries AD: insights from the pottery waste[J/OL]. *Archaeological and Anthropological Sciences*, 2020, 12(9): 221. <https://link.springer.com/10.1007/s12520-020-01113-2>. DOI: <https://www.doi.org/10.1007/s12520-020-01113-2>.
- [7] Ramírez Argáez M A, Huacúz S L, Trápaga G. Mathematical Modeling of Pottery Production in Different Industrial Furnaces[J/OL]. *Journal of Materials Engineering and Performance*, 2008, 17(5): 633-643. <http://link.springer.com/10.1007/s11665-008-9217-5>. DOI: <https://www.doi.org/10.1007/s11665-008-9217-5>.
- [8] Nilenius K. CFD simulation of flue gas flow in traditional Indonesian pottery furnace.[C/OL]// Nilenius2011CFDSO. 2011. <https://publications.lib.chalmers.se/records/fulltext/147675.pdf>.
- [9] Awaji H, Watanabe T, Nagano Y. Compressive testing of ceramics[J/OL]. *Ceramics International*, 1994, 20(3): 159-167. <https://linkinghub.elsevier.com/retrieve/pii/0272884294900345>. DOI: [https://www.doi.org/10.1016/0272-8842\(94\)90034-5](https://www.doi.org/10.1016/0272-8842(94)90034-5).
- [10] Moustafa T, Azmy A, El-sakka A, et al. Cold Flow Numerical Simulation Inside Local Pottery Furnace for Different Designs for the Air Inlet[J/OL]. 2019 Novel Intelligent and Leading Emerging Sciences Conference (NILES), 2019, 1(3): 178-181. <https://ieeexplore.ieee.org/document/8909323/>. DOI: <https://www.doi.org/10.1109/NILES.2019.8909323>.
- [11] Ravi M R, Dhar P L, Kohli S. Energy Audit and Improvement of an Updraught Pottery Kiln[J]. *Sesi*, 2007, 17: 1-20.
- [12] Govind K. Design and Simulation of Pottery Kiln[J].
- [13] CFD Online. Standard k-epsilon model[EB/OL]. 2014[8 July 2021]. https://www.cfd-online.com/Wiki/Standard_k-epsilon_model.
- [14] Jiyuan T, Guan Heng Y, Chaoqun L. Computational fluid dynamics[M/OL]. 2nd ed. Butterworth Heinemann, 2012: 456. <https://www.elsevier.com/books/computational-fluid-dynamics/tu/978-0-08-098243-4>.